

Sintering and crystallization of off-stoichiometric $\text{BaO}\cdot\text{Al}_2\text{O}_3\cdot 2\text{SiO}_2$ glasses

YUN-MO SUNG*, JAE-WOO AHN

Department of Materials Science and Engineering, Daejin University, Pocheon-koon, Kyunggi-do 487-711, South Korea

E-mail: ymsung@road.daejin.ac.kr

Glass-ceramics with off-stoichiometric celsian composition of 50 wt% $\text{BaO}\cdot 2\text{SiO}_2$ – 50 wt% $\text{BaO}\cdot\text{Al}_2\text{O}_3\cdot 2\text{SiO}_2$, (B2S-BA2S) were fabricated and investigated for their sintering and crystallization characteristics. (B2S-BA2S) glass powder showed a melting temperature much lowered compared to that of stoichiometric $\text{BaO}\cdot\text{Al}_2\text{O}_3\cdot 2\text{SiO}_2$ (BA2S) glass powder and high sintering ability. (B2S-BA2S) glass powder containing B_2O_3 , (B2S-BA2S)B and that containing B_2O_3 and TiO_2 , (B2S-BA2S)BT revealed much lowered crystallization peak temperatures, but rather low sintered density. By applying Kissinger analysis to differential thermal analysis (DTA) data activation energy values for crystallization were determined as 265, 195 and 242 kJ/mol, respectively for (B2S-BA2S), (B2S-BA2S)B and (B2S-BA2S)BT glasses. X-ray diffraction (XRD) patterns from all the glass-ceramics crystallized at 1100°C for 4 h revealed formation of crystalline phases of β - $\text{BaO}\cdot 2\text{SiO}_2$, monocelsian and hexacelsian. (B2S-BA2S) glass-ceramics crystallized at 1400°C for 4 h showed formation of β - $\text{BaO}\cdot 2\text{SiO}_2$ and monocelsian phases with only trace of metastable hexacelsian phase.

© 2000 Kluwer Academic Publishers

1. Introduction

Glass-ceramics have been used for various purposes including high-temperature structural applications and electronic packaging due to their unique properties such as high strength, low density, chemical stability, low thermal expansion and low dielectric properties [1]. Sintering of glass powder followed by crystallization of the glass body can give huge benefit to glass-ceramic fabrication since this method can reduce processing temperature and make the fabrication of complex-shape components possible using variety of conventional ceramic forming techniques [2–11].

Barium aluminosilicate composition of $\text{BaO}\cdot\text{Al}_2\text{O}_3\cdot 2\text{SiO}_2$ (BA2S) forming monoclinic celsian (monocelsian) as a primary crystalline phase, has been studied mainly for the use as matrix materials for high-temperature ceramic composites [12, 13]. Major reasons of this include its high melting point of $\sim 1760^\circ\text{C}$, low thermal coefficient expansion (TCE) of $\sim 2.29 \times 10^{-6}/^\circ\text{C}$, oxidation resistance and phase stability up to $\sim 1590^\circ\text{C}$ [14, 15]. Another high-temperature form in BA2S system is hexacelsian phase which is stable above 1590°C , metastably existing down to room temperature. Hexacelsian shows relatively high thermal expansion ($\sim 8.0 \times 10^{-6}/^\circ\text{C}$) and undergoes reversible displacive transformation to an orthorhombic form, followed by large volume change ($\sim 3\%$). Thus, formation of hexacelsian phase in BA2S system is undesirable in structural applications.

According to Hyatt and Bansal [15] metastable hexacelsian always crystallizes first during heating the BA2S glass and transformation from hexacelsian to monocelsian is very sluggish. They prepared BA2S glass powder by melting at 2000°C and attrition milling, and reported that BA2S glass powder heated at 1000°C for 1 h was completely crystallized to pure hexacelsian phase and those heated at 1100°C for 10 h began to transform to monocelsian. BA2S glass powder heated even at 1400°C for 10 h showed formation of both hexacelsian and monocelsian phases although the amount of monocelsian phase was increased relative to hexacelsian.

Sung *et al.* [8–10] prepared off-stoichiometric strontium-celsian glass-ceramics, $(\text{SrO}\cdot\text{SiO}_2)\text{-(SrO}\cdot\text{Al}_2\text{O}_3\cdot 2\text{SiO}_2)$ and $(\text{SrO}\cdot\text{Al}_2\text{O}_3\cdot 2\text{SiO}_2)\text{-(Al}_2\text{O}_3)$ with and without additives of B_2O_3 , P_2O_5 and/or TiO_2 . The former showed formation of equilibrium $\text{SrO}\cdot\text{SiO}_2$ and monocelsian phases while the latter with B_2O_3 showed formation of only monocelsian phase. They showed high sintering ability and mechanical properties suitable for applications in composite matrices [11] and heat exchanger parts as well as reduced processing temperatures and time periods.

In this study, off-stoichiometric BA2S composition was selected for glass-ceramic fabrication since the melting temperature of 2000°C is too high for real applications. Glass-ceramics with off-stoichiometric binary join composition of 50 wt% ($\text{BaO}\cdot 2\text{SiO}_2$) – 50 wt%

* Author to whom all correspondence should be addressed.

(BaO·Al₂O₃·2SiO₂) (B2S-BA2S), were produced by cold pressing and sintering of glass powder followed by crystallization heat treatments. Their sintering and crystallization behavior was compared with that of stoichiometric BA2S glass-ceramics studied by previous researchers. Also, the effect of sintering aid (B₂O₃) and nucleation agent (TiO₂) on sintering and crystallization behavior of off-stoichiometric (B2S-BA2S) glass-ceramics was studied in detail.

2. Experimental procedures

High purity oxides of BaCO₃, Al₂O₃, SiO₂, B₂O₃ and TiO₂ from Aldrich Chemical (Milwaukee, WI, USA) were used as starting materials. Table I lists the composition of each glass prepared for the present study. (B2S-BA2S) composition indicating 50 wt% BaO·2SiO₂—50 wt% BaO·Al₂O₃·2SiO₂ corresponds to 48.45 wt% BaO, 13.58 wt% Al₂O₃ and 37.97 wt% SiO₂. Each powder was well mixed using zirconia-ball milling. Powder mixture was loaded in a platinum crucible and placed inside a resistance furnace with super Kanthal[®] heating elements for glass melting. The weight of glass batch was 20 g. The powder mixture was heated to 1000°C for 1 h for calcination and further heated to 1600°C for 1 h for complete glass melting. The platinum crucible containing glass melt was quenched into distilled water and clear glass fragments were obtained. Glass fragments were dried and hand ground using a high-purity alumina mortar and pestle. The hand-ground glass powder was zirconia-ball milled to the average particle size of 3–5 μm. Each of the glass powder was analyzed for various temperatures such as glass transition (*T_g*), crystallization onset (*T_o*) and crystallization peak (*T_p*) using differential thermal analyses (DTA: SETARAM TGDTA-92, France). DTA results were further analyzed for activation energy for crystallization using Kissinger analysis.

Fine glass powder was pelletized using a steel die and a hydraulic press under 3000 psi at room temperature. Glass pellets were 4 mm in diameter and 2 mm in thickness. The cold-pressed pellets loaded in a platinum cup were brought to the DTA for sintering and rate-heated (20°C/min) to 850°C for (B2S-BA2S) and 800°C for (B2S-BA2S)B and (B2S-BA2S)BT glasses which temperatures are between *T_g* and *T_o*. The sintered glass pellets were further heated for crystallization at 1100°C which is above *T_p*'s. Duration at each of the sintering and crystallization temperatures was 2 and 4 h, respectively and was performed in air. The glass-ceramic pellets were analyzed for density using the Archimedes principle. The glass-ceramic pellets were cut in the middle by using a low-speed diamond saw and mounted in

TABLE I Compositions of the glasses prepared for the present study

Glasses	Components (wt%)				
	BaO	Al ₂ O ₃	SiO ₂	B ₂ O ₃	TiO ₂
(B2S-BA2S)	48.45	13.58	37.97	—	—
(B2S-BA2S)B	47.00	13.17	36.83	3.00	—
(B2S-BA2S)BT	45.54	12.77	35.69	3.00	3.00

epoxy resin. The cross sections of the glass-ceramic pellets were polished and gold coated. Scanning electron microscopy (SEM: JSM-6100, Jeol, Japan) was performed on the samples to examine microstructure of the glass-ceramics. X-ray diffraction (XRD: Nicolet Stoe Transmission/Bragg-Brentano, Stoe Co., Germany) was also performed on the powdered glass-ceramics with a Cu-K_α source, a 2-s time constant, a 10–60° scan, and 0.02° step size. Phase identification was done by comparison of peak locations and intensities with the data listed in JCPDS cards (#38-1450 for monocelsian, #26-137 for hexacelsian and #26-176 for BaO·2SiO₂).

3. Results

(B2S-BA2S), (B2S-BA2S)B and (B2S-BA2S)BT compositions were completely melted to form homogeneous glass melts at 1600°C. By using XRD analyses clear non-crystallinity was identified for the three glasses. Glass transition and crystallization trends of the glasses were investigated using DTA. DTA scan curves from the three glasses at the heating rates of 10, 15, 20, 30 and 40°C/min are shown in Figs 1–3. All of the three off-stoichiometric glasses showed double

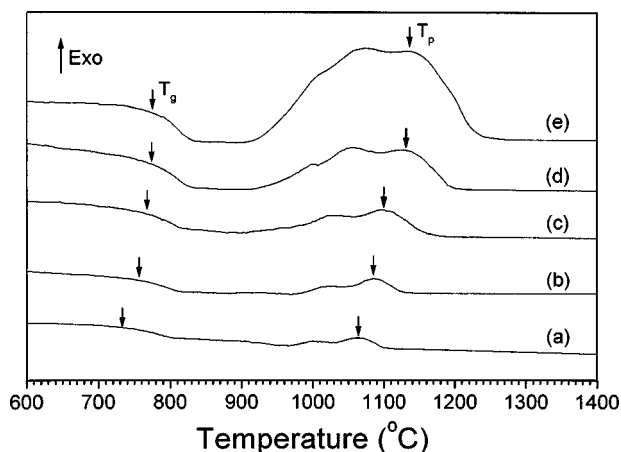


Figure 1 Differential thermal analysis (DTA) scan curves of (B2S-BA2S) glass. Each of the scan curves corresponds to scan rates of (a) 10, (b) 15, (c) 20, (d) 30 and (e) 40°C/min, respectively.

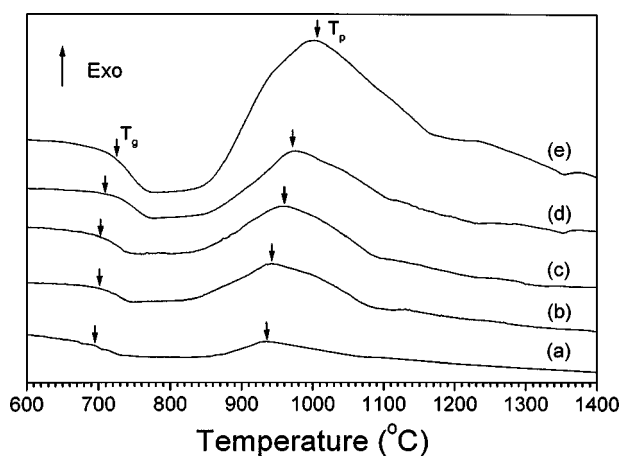


Figure 2 Differential thermal analysis (DTA) scan curves of (B2S-BA2S)B glass. Each of the scan curves corresponds to scan rates of (a) 10, (b) 15, (c) 20, (d) 30 and (e) 40°C/min, respectively.

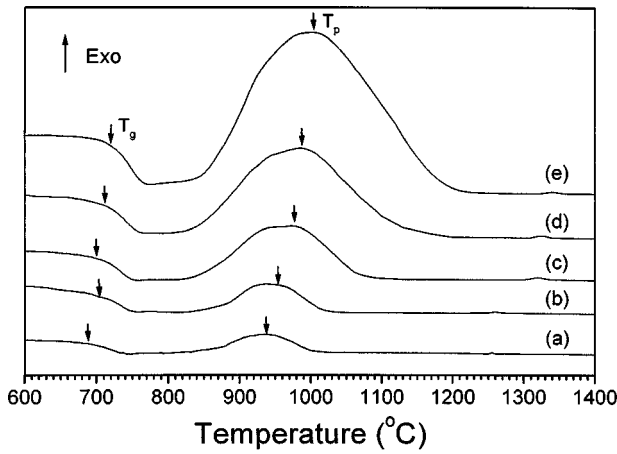


Figure 3 Differential thermal analysis (DTA) scan curves of (B2S-BA2S)BT glass. Each of the scan curves corresponds to scan rates of (a) 10, (b) 15, (c) 20, (d) 30 and (e) 40°C/min, respectively.

crystallization peaks. To identify each of the two peaks, glass powder was DTA rate heated (20°C/min) just above crystallization onset temperature (T_o) and cooled to room temperature at the highest cooling rate (~90°C/min). XRD analyses on the heated samples revealed distinct crystalline peaks from β -BaO·2SiO₂ crystals with the broad hill from remaining glass phase. Other crystalline phases were not observed in the XRD patterns. Thus, the first peak in the DTA curves was identified to correspond to crystallization of glass to β -BaO·2SiO₂ phase and the second one glass to hexacelsian phase. Table II lists T_g and T_p values of different glasses at various scan rates. For non-stoichiometric glasses T_p values correspond to crystallization temperatures of hexacelsian phase. The temperature values for stoichiometric BA2S glass were taken from Hyatt and Bansal's data [15]. Off-stoichiometric (B2S-BA2S) glass shows a T_p value higher than that of stoichiometric BA2S glass. The other off-stoichiometric glasses, (B2S-BA2S)B and (B2S-BA2S)BT, show T_p values lower than that of (B2S-BA2S) glass. Unexpectedly, (B2S-BA2S)B glass showed lower T_p value than (B2S-BA2S)BT glass.

For the DTA scan curves, the faster the heating rates, the higher the peak temperatures and the larger the peak heights become [6, 7]. The variation in T_p with DTA scan rates can be used to estimate activation energy for crystallization [16] by using following Kissinger analysis [17].

$$\ln\left(\frac{\phi}{T_p^2}\right) = -\frac{E_{ck}}{RT_p} + \text{const.} \quad (1)$$

TABLE II Summary of glass transition (T_g) and crystallization peak (T_p) temperatures of glasses prepared for the present study

Glasses	Glass transition temp. (°C)					Crystallization peak temp. (°C)				
	DTA scan rates (°C/min)					DTA scan rates (°C/min)				
	10	15	20	30	40	10	15	20	30	40
BA2S*	879	—	892	895	907	1053	—	1071	1086	1098
(B2S-BA2S)	733	756	766	774	774	1063	1085	1098	1126	1135
(B2S-BA2S)B	695	704	705	708	723	938	942	959	961	1002
(B2S-BA2S)BT	687	707	700	716	720	935	953	975	984	1000

*The T_g and T_p values of the BA2S glass are taken from Hyatt and Bansal's DSC data [15].

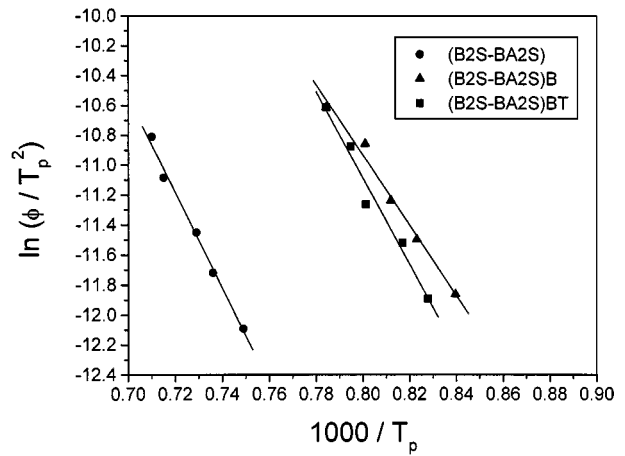


Figure 4 Kissinger plots of (B2S-BA2S), (B2S-BA2S)B and (B2S-BA2S)BT glasses. From slopes of the curves activation energy values for crystallization were determined as 265, 195 and 242 kJ/mol, respectively.

where ϕ is the DTA scan rate (°C/min), T_p is the crystallization peak temperature (°K), E_{ck} is the activation energy (kJ/mol) for the crystallization from Kissinger equation and R is the gas constant (8.3144 J/mol°K). Fig. 4 shows Kissinger plots of various glasses. The activation energy for crystallization (E_{ck}) can be determined from the slope ($-E_{ck}/R$) of each Kissinger plot. Activation energy values for (B2S-BA2S), (B2S-BA2S)B and (B2S-BA2S)BT glasses, were determined to be 265, 195 and 242 kJ/mol, respectively.

Glass-ceramic pellets sintered at 850 or 800°C for 2 h and crystallized at 1100°C for 4 h, were analyzed for density using the Archimedes method. Density value of (B2S-BA2S) glass-ceramic pellet was determined as 3.47 g/cm³ while those of (B2S-BA2S)B and (B2S-BA2S)BT glass-ceramic pellets were determined to be 3.29 and 3.33 g/cm³, respectively.

Scanning electron micrographs (SEM) of glass-ceramics are shown in Fig. 5a-c. Microstructure of (B2S-BA2S) glass-ceramic showed low porosity while that of (B2S-BA2S)B and (B2S-BA2S)BT glass-ceramics showed relatively high porosity. This microstructural analysis well corresponds to density measurements.

XRD patterns from (B2S-BA2S), (B2S-BA2S)B and (B2S-BA2S)BT glass-ceramics sintered and crystallized were almost identical and showed formation of crystalline phases of β -BaO·2SiO₂, hexacelsian and monocelsian. Fig. 6a shows XRD patterns from powdered (B2S-BA2S) glass-ceramics crystallized at

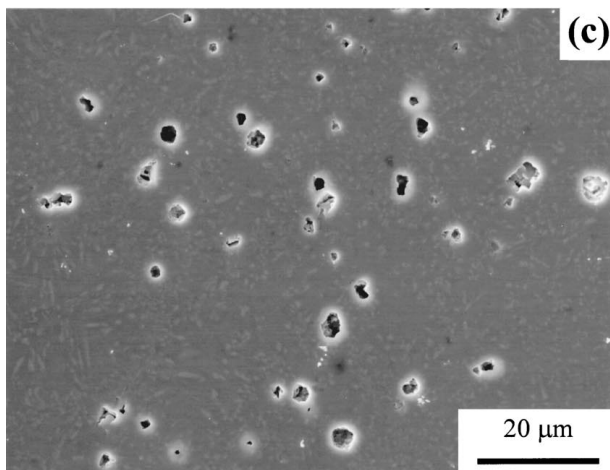
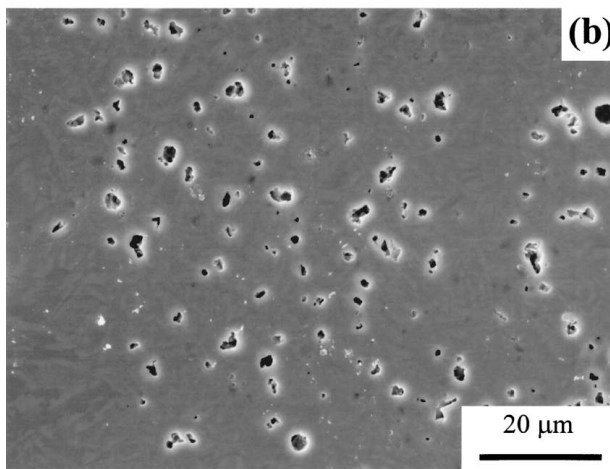
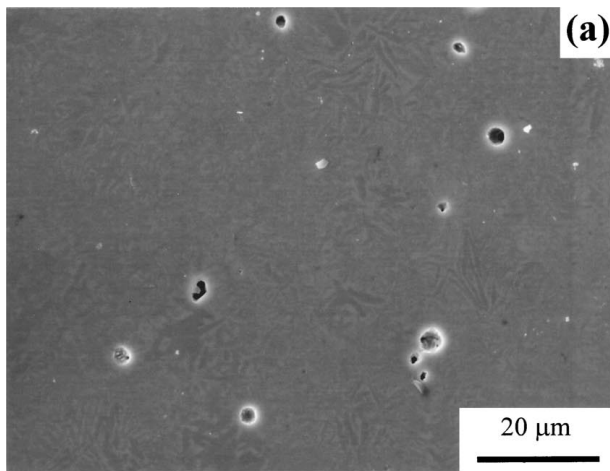


Figure 5 Scanning electron micrographs (SEM) of (a) (B2S-BA2S), (b) (B2S-BA2S)B and (c) (B2S-BA2S)BT glass-ceramics sintered at 850 or 800°C for 2 h and crystallized at 1100°C for 4 h.

1100°C for 4 h. Intensities of monocelsian peaks were strong. XRD patterns for glass-ceramics heated at 1400°C for 4 h showed formation of β -BaO·2SiO₂ and monocelsian with only trace of hexacelsian as shown in Fig. 6b.

4. Discussion

Glass transition and crystallization behavior of a glass can give the key information to the glass-ceramic fabrication. According to the Hyatt and Bansal's DSC data

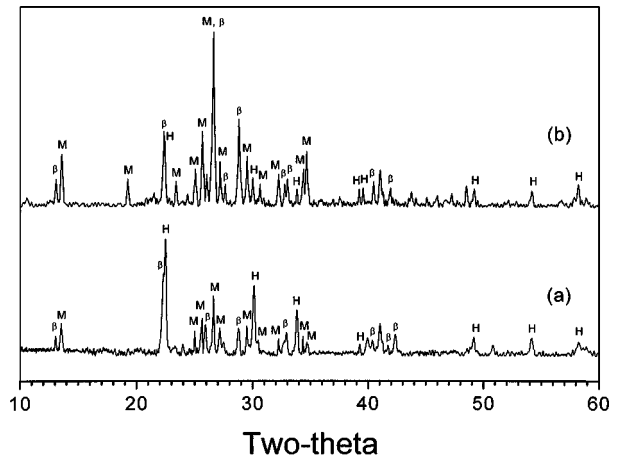


Figure 6 X-ray diffraction (XRD) patterns of (a) (B2S-BA2S) glass-ceramics crystallized at 1100°C for 4 h showing formation of equilibrium phases of β -BaO·2SiO₂ (β), hexacelsian (H) and monocelsian (M) and (b) (B2S-BA2S) glass-ceramics crystallized at 1400°C for 4 h showing trace of hexacelsian phase.

[15] glass transition temperature (T_g) of stoichiometric BA2S celsian with a scan rate of 20°C/min, was 892°C while those of glasses prepared for the present study, (B2S-BA2S), (B2S-BA2S)B and (B2S-BA2S)BT, were 776, 705 and 710°C, respectively. Lowered glass transition implies decrease in the number of ionic bonds and/or formation of weak ionic bonds in a glass. The effect of a sintering aid of B₂O₃ is very clear since (B2S-BA2S)B and (B2S-BA2S)BT glasses show T_g lowered by 71 and 66°C, respectively compared to (B2S-BA2S) glass. The addition of B₂O₃ could reduce strong connectivity of the three-dimensional chain structure of a barium aluminosilicate glass and also create weak ionic bonds thus, can lower its glass transition temperature. This is most probable since B₂O₃ has only two-dimensional chain structure consisting of connected hexagonal rings and the bonds connecting the hexagonal rings are very weak.

Crystallization peak temperature (T_p) of stoichiometric BA2S glass with a scan rate of 20°C/min was 1071°C while those of (B2S-BA2S), (B2S-BA2S)B and (B2S-BA2S)BT glasses were 1098, 959 and 972°C, respectively. Crystallization of a glass can take place by rearrangement of ions randomly oriented in it thus, diffusion process is involved. Since (B2S-BA2S)B and (B2S-BA2S)BT glasses most probably have lower connectivity between ions and they have relatively weak ionic bonds as well they can readily crystallize and thus, have lower crystallization peak temperatures (T_p 's) compared to (B2S-BA2S) glass. The addition of nucleation agent, TiO₂, seems not to be effective since T_p of (B2S-BA2S)BT is higher than that of (B2S-BA2S)B glasses.

A careful look at the DTA curves of a glass reveals that there are two crystallization peaks. By XRD analyses on the samples quenched right after heated to crystallization onset temperatures (T_o) it was identified that the first peak corresponds to crystallization of a part of the glass to β -BaO·2SiO₂ phase. The incorporation of sintering aid, B₂O₃ into a glass seems to enhance crystallization considerably by reducing the number

of three-dimensional ionic bonds and formation weak ionic bonds. Since crystallization occurs by diffusion of ions this situation would have enhanced the crystallization. Both the first and second peak temperatures lowered by more than 100°C. Thus, the addition of B₂O₃ enhanced crystallization of both the β -BaO·2SiO₂ and hexacelsian phases. However, nucleation agent, TiO₂ seems not to work since peak temperatures of (B2S-BA2S)BT glass were slightly higher than those of (B2S-BA2S)B glass. In the case of these glass-ceramics low ionic connectivity and weak ionic bonds most likely plays a major role in determining the crystallization behavior instead of the precursor nuclei such as titanates.

The activation energy values for crystallization of hexacelsian phase obtained by using the Kissinger method indicate that glasses prepared for the present study have much lower values (265, 195 and 242 kJ/mol) than that (560 kJ/mol) of stoichiometric BA2S glass [15]. This difference would occur since for (B2S-BA2S), (B2S-BA2S)B and (B2S-BA2S)BT glasses pre-existing β -BaO·2SiO₂ crystals can act as heterogeneous nucleation sites for the formation of hexacelsian phase. The reason that (B2S-BA2S)B and (B2S-BA2S)BT glasses have lower activation energy values than (B2S-BA2S) glass would be explained by low ionic connectivity and weak ionic bonds of the glass remained after forming the β -BaO·2SiO₂ crystals. This condition of the remaining glass also would come from the B₂O₃ addition.

Density value of (B2S-SA2S) glass-ceramic was high while those of (B2S-BA2S)B and (B2S-BA2S)BT glass-ceramics were low. The sintering ability of a glass can be estimated from the temperature range between crystallization onset and glass transition, ($T_0 - T_g$). The viscosity of a glass rapidly decreases when heated above T_g at which glass chain structure is broken, and then dramatically increase when crystallization initiates since ions start to form highly ordered crystalline structure. Thus, sintering of a glass occurs at the temperature range of $T_0 - T_g$. If the temperature range is small a premature crystallization can occur before the completion of the sintering. Once premature crystallization occurs viscosity of a glass increases tremendously and sintering terminates. Thus, high sintering ability can not be expected from a glass with small temperature range of $T_0 - T_g$. For (B2S-BA2S), (B2S-BA2S)B and (B2S-BA2S)BT glasses T_0 corresponds to crystallization onset temperature of the β -BaO·2SiO₂ phase. The $T_0 - T_g$ values of each glass are 183, 130 and 148°C, respectively. This result is in good agreement with the density data.

The theoretical density value of glass-ceramics can be determined by using each theoretical density value of the β -BaO·2SiO₂ (3.77 g/cm³), hexacelsian (3.268 g/cm³) and monocelsian (3.39 g/cm³) crystals, and mol% of each phase. The weight percentage (50 wt% BaO·2SiO₂ – 50 wt% BaO·Al₂O₃·2SiO₂) of glass-ceramics can be converted to molar percentage (57.86 mol% BaO·2SiO₂ – 42.14 mol% BaO·Al₂O₃·2SiO₂). Assuming that BA2S consists of 50 mol% hexacelsian and 50 mol% monocelsian the theoretical density of (B2S-BA2S) glass-ceramic thus, would be estimated as 3.584 g/cm³. Therefore, (B2S-BA2S),

(B2S-BA2S)B and (B2S-BA2S)BT glass-ceramic pellets respectively show 97, 92 and 93% of its theoretical density. In considering the fact that these glass-ceramics were fabricated using only pressureless sintering after cold pressing, sintering ability of (B2S-BA2S) glass-ceramic is relatively high. Although addition of B₂O₃ considerably lowered crystallization temperatures of glasses it caused premature crystallization which resulted in low sintered density. This can be evidenced by the small $T_0 - T_g$ values in the glasses containing B₂O₃.

SEM micrographs on the glass-ceramics well support density measurements and DTA results. (B2S-BA2S)B and (B2S-BA2S)BT glass-ceramics showed relatively high porosity compared to (B2S-BA2S) glass-ceramic. The contrasted texture micrographs comes from component difference between β -BaO·2SiO₂ and BO·Al₂O₃·2SiO₂ phases. The former is brighter since it contains higher content of heavy barium ions.

All the XRD patterns on the three glass-ceramics crystallized at 1100°C for 4 h were almost identical and showed formation of equilibrium phases of β -BaO·2SiO₂ and monocelsian and a metastable phase of hexacelsian. No trend of non-crystallinity was found in the XRD patterns. Both hexacelsian and monocelsian phases were identified for BO·Al₂O₃·2SiO₂. Glass-ceramics showed formation of monocelsian phase with much shorter time period compared to stoichiometric BA2S glass-ceramics. XRD patterns on (B2S-BA2S) glass-ceramics crystallized at 1400°C for 4 h showed high peak intensities of monocelsian phase with much lowered peak intensities of hexacelsian phase. Formation of monocelsian phase in off-stoichiometric glasses was also enhanced compared to stoichiometric BA2S glasses.

5. Conclusions

To develop a glass-ceramic material with low processing temperatures and high sintering ability off-stoichiometric (B2S-BA2S) compositions were studied for sintering and crystallization behavior. (B2S-BA2S) composition showed melting temperature lowered by ~260°C compared to the stoichiometric BA2S composition. Due to decrease in the number of ionic bonds and formation of weak ionic bonds (B2S-BA2S)B and (B2S-BA2S)BT glasses showed approximately 100°C lowered crystallization peak temperature compared to (B2S-BA2S) glass. Also, most likely due to pre-existing β -BaO·2SiO₂ crystals in a glass matrix (B2S-BA2S), (B2S-BA2S)B and (B2S-BA2S)BT glasses showed much lower activation energy values for crystallization than that of the stoichiometric BA2S glass. (B2S-BA2S) glass has the biggest temperature range of $T_0 - T_g$ and thus, showed the highest density (97% of the theoretical density) among the three glasses. XRD patterns from off-stoichiometric BA2S glass-ceramics revealed formation of three crystalline phases of β -BaO·2SiO₂, hexacelsian and monoclesian phases. In light of low processing temperature and high sintering ability (B2S-BA2S) glass-ceramics have high potential to be used for variety of applications.

Acknowledgements

The authors wish to thank Mr. Bum-Ho Jung at Daejin University for helping DTA work. This study was supported by the Daejin University Research Grants of 1998.

References

1. G. H. BEALL and D. A. DUKE, in "Glass Science and Technology, Vol. 1: Glass-Ceramic Technology," edited by D. R. Uhlmann and N. J. Kreidl (Academic Press, New York, 1983) p. 403.
2. E. M. RABINOVICH, in "Advances in Ceramics, Vol. 4: Nucleation and Crystallization in Glasses," edited by J. H. Simmons, D. R. Uhlmann and G. H. Beall (American Ceramic Society, Columbus, OH, 1982) p. 327.
3. P. C. PANDA, W. M. MOBLEY and R. RAJ, *J. Am. Ceram. Soc.* **72** (1989) 2361.
4. T. RUDOLPH, K-L. WEISSKOPT, W. PANNHORST and G. PETZOW, *Glasstech. Ber.* **64** (1991) 305.
5. S. KNICKERBOCKER, M. R. TUZZOLO and S. LAWHORNE, *J. Am. Ceram. Soc.* **72** (1989) 1873.
6. Y.-M. SUNG, S. A. DUNN and J. A. KOUTSKY, *J. Eur. Ceram. Soc.* **14** (1994) 455.
7. Y.-M. SUNG, *J. Mater. Sci.* **31** (1996) 5421.
8. Y.-M. SUNG and J. S. PARK, *ibid.* **34** (1999) 5803.
9. Y.-M. SUNG, *J. Mater. Sci. Lett.* **18** (1999) 1229.
10. Y.-M. SUNG and S. KIM, *J. Mater. Sci.*, in press (2000).
11. Y.-M. SUNG, *J. Mater. Sci. Lett.* **18** (1999) 1315.
12. N. P. BANSAL, U.S. Patent 5214004 (1993).
13. *Idem.*, *Mater. Sci. & Eng.* **A220** (1996) 129.
14. C. H. DRUMMOND III and N. P. BANSAL, *Ceram. Eng. Sci. Proc.* **11** (1990) 1072.
15. M. J. HYATT and N. P. BANSAL, *J. Mater. Sci.* **31** (1996) 172.
16. Y.-M. SUNG and J.-H. SUNG, *ibid.* **33** (1998) 4733.
17. H. E. KISSINGER, *J. Res. Natl. Bur. Stand. (US)* **57** (1956) 217.

*Received 23 April 1999
and accepted 28 March 2000*